Fig. S1

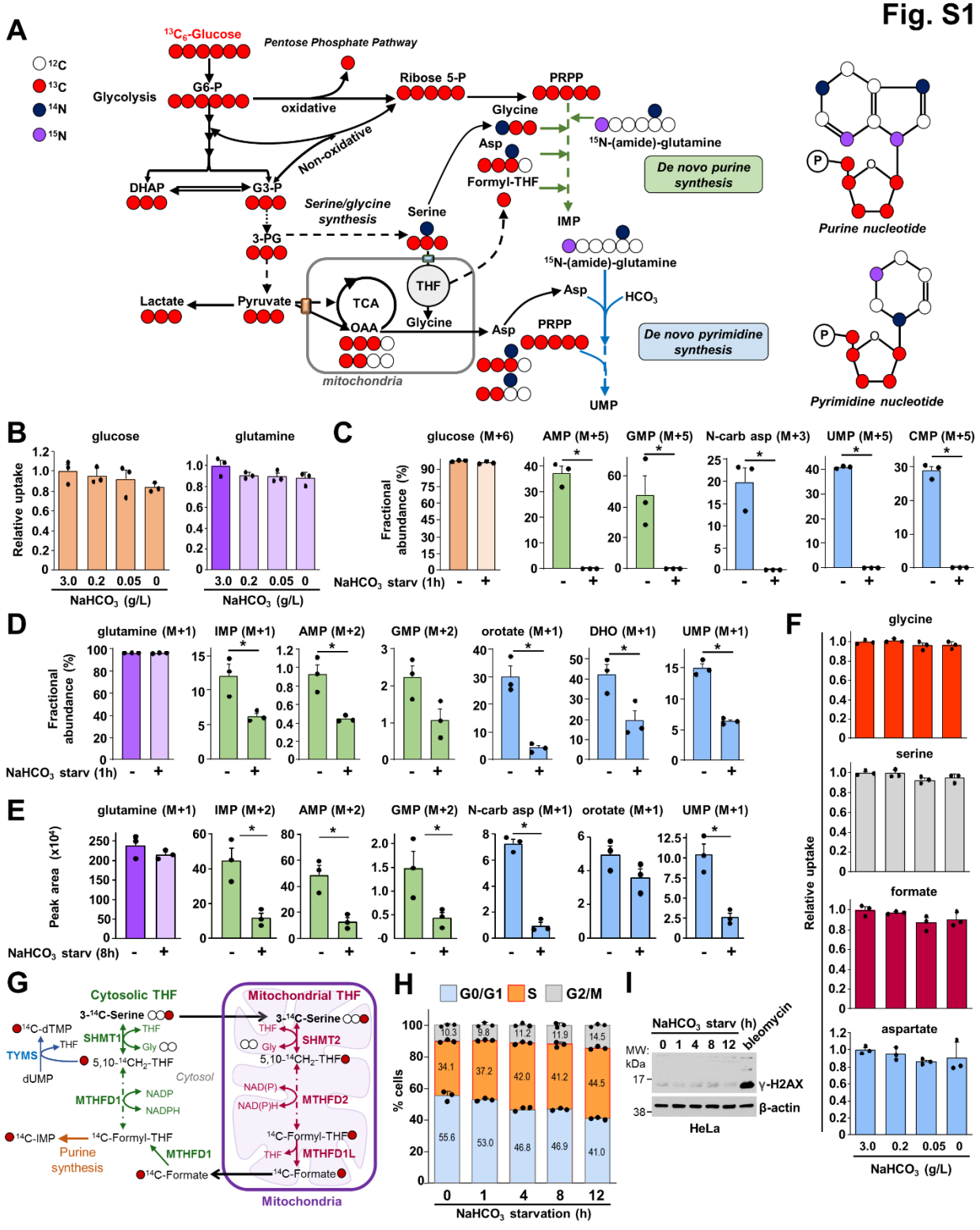

Figure S1. Bicarbonate levels control de novo nucleotide synthesis. Related to Figure 1.

(A) Schematic of $^{13}C_6$-glucose and ^{15}N-(amide)-glutamine labeling into purine and pyrimidine nucleotides.

(B) Uptake of glucose and glutamine monitored in response to bicarbonate starvation. HeLa cells were cultured in dialyzed serum and were subjected to different concentration of $NaHCO_3$ for 1h and labeled with ^{3}H-2-deoxyglucose or $^{14}C_5$-glutamine over the last 5 min. The CPM values were normalized to the protein concentration and uptake duration. Relative levels are shown. The data are presented as the means ± SDs of two independent experiments.

(C) Fractional abundance of ^{13}C-labeled metabolite intermediates, as measured by targeted LC-MS/MS, in HeLa cells grown in dialyzed serum and depleted of $NaHCO_3$ for 1 h and labeled with $^{13}C_6$-glucose for 1 h. These data support the stable-isotope tracing experiments presented in Figure 1D.

(D) Fractional abundance of ^{15}N-labeled metabolite intermediates, as measured as in C, in HeLa cells grown in dialyzed serum and depleted of $NaHCO_3$ for 1 h and labeled with ^{15}N-(amide)-glutamine for 1 h. These data support the stable-isotope tracing experiments presented in Figure 1E.

(E) Peak areas of ^{15}N-labeled metabolite intermediates, as measured as in C, in HeLa cells grown in dialyzed serum and depleted of $NaHCO_3$ for 8 h and labeled with ^{15}N-(amide)-glutamine for the final hour.

(F) Uptake of glycine, serine, formate and aspartate in response to different concentrations of bicarbonate. HeLa cells were subjected to different concentrations of $NaHCO_3$ for 1 h and labeled with ^{14}C-glycine, ^{14}C-serine, ^{14}C-formate or ^{14}C-aspartate for the last 5 min. The CPM values were normalized to the protein concentration and uptake duration. Relative levels are shown. The data are presented as the means ± SDs of two independent experiments.

(G) Illustration of the fate of the 3-position carbon of serine into one-carbon metabolism, purine, and deoxythymidylate synthesis.

(H) Cell cycle analysis of HeLa cells cultured in buffered DMEM medium (20 mM HEPES) in the presence or absence of sodium bicarbonate ($NaHCO_3$) over the indicated times.

(I) Immunoblots of HeLa cells treated as in H. Treatment with Bleomycin (10 μM, 8 h) was used as positive control to induce γ-H2AX phosphorylation.

(B)-(I) The data are graphed as the means ± SDs of biological triplicates and are representative of at least two independent experiments. $*p < 0.05$ was calculated by two-tailed Student's t-test for pairwise comparisons (C-E).

Fig. S2

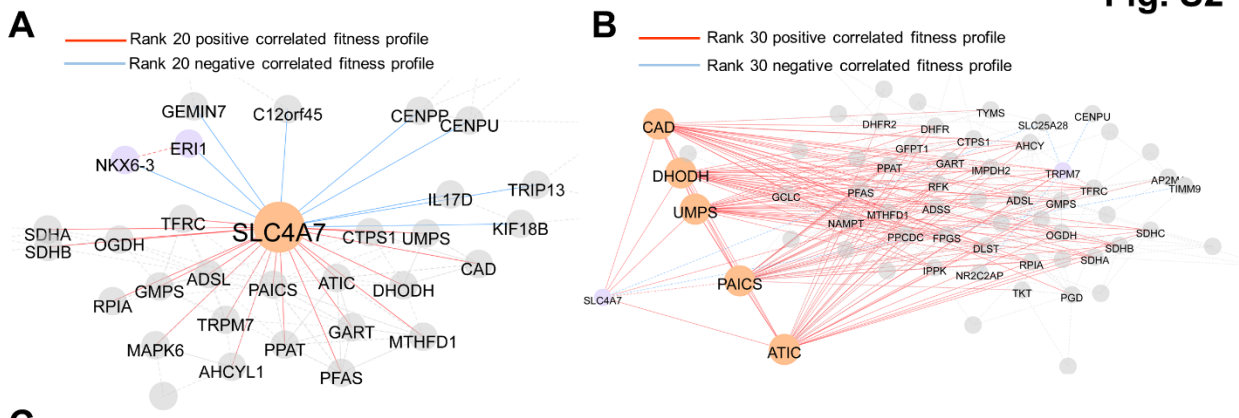

C

SLC4A gene family	Gene (dependent)	Entrez Id	Pearson correlation
SLC4A1	SOST	50964	0.19
	G6PC3	92579	0.19
	HOXB2	3212	0.18
	ITGA2B	3674	0.18
	GRN	2896	0.18
SLC4A2	GIMAP4	55303	0.19
	KIDINS220	57498	0.17
	FAF2	23197	0.16
	FAM13B	51306	0.16
	WEE2	494551	0.16
SLC4A3	CFAP65	255101	0.18
	DNAJB2	3300	0.18
	SPEG	10290	0.18
	PRLH	51052	0.17
	ASIC4	55515	0.17
SLC4A4	UGT2A1	10941	0.20
	ENOPH1	58478	0.18
	TNN	63923	-0.18
	FAM47E	100129583	0.18
	CASP6	839	0.17
SLC4A5	DOK1	1796	0.19
	SFTPB	6439	0.19
	ZBTB8OS	339487	0.18
	ARID5A	10865	0.18
	ELMOD3	84173	0.18
SLC4A7	UMPS	7372	0.40
	AHCYL1	10768	0.40
	TRPM7	54822	0.40
	CAD	790	0.38
	GMPS	8833	0.37
SLC4A8	POU6F1	5463	0.35
	TMPRSS12	283471	0.35
	VDR	7421	0.30
	PRPF40B	25766	0.29
	ASIC1	41	0.29
SLC4A9	NRG2	9542	0.22
	SLC22A5	6584	0.21
	CAMK2A	815	0.20
	SLC23A1	9963	0.17
	SIL1	64374	0.17
SLC4A10	CACNB4	785	0.24
	GALNT5	11227	0.21
	NEB	4703	0.20
	MAP3K20	51776	0.19
	MITD1	129531	0.18
SLC4A11	AVP	551	0.30
	MAVS	57506	0.28
	SPEF1	25876	0.27
	HSPA12B	116835	0.27
	GFRA4	64096	0.25

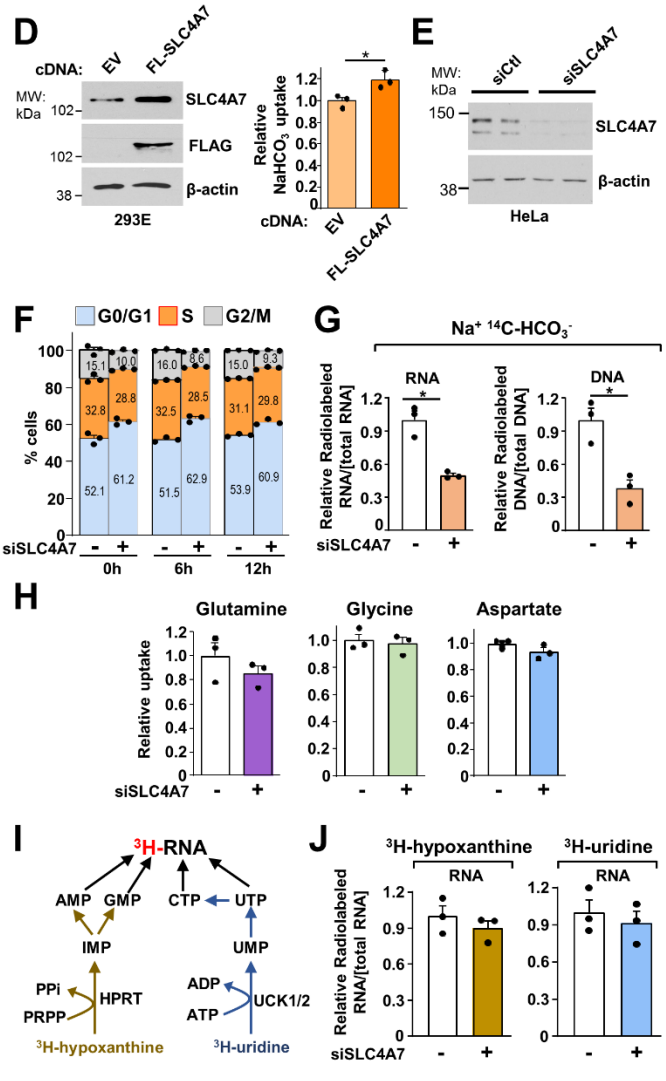

Figure S2. The sodium bicarbonate SLC4A7 shows gene coessentiality with de novo nucleotide metabolism. Related to Figure 2.

(A) The *SLC4A7* coessentiality network reveals enrichment for the de novo nucleotide synthesis pathways.

(B) Co-essentiality network of de novo purine and pyrimidine enzymes demonstrates the positive correlation fitness with the *SLC4A7* gene.

(C) Top 5 Co-dependencies from genome wide CRISPR knockout screens (DepMap 22Q1 Public+Score, Chronos) for the bicarbonate transporters.

(D) Immunoblots of HEK293E cells transfected with either empty vector or FLAG-SLC4A7 for 48 h. The HEK293E-transfected cells were incubated with Na+, ^{14}C-HCO_3^- for 5 min to measure bicarbonate uptake.

(E) Immunoblots of wild-type HeLa cells grown in 10 % serum and transfected with siRNA targeting SLC4A7 or nontargeting controls for 48 h.

(F) Cell cycle analysis of HeLa cells transfected with siRNA targeting SLC4A7 or nontargeting controls for 48 h and subjected to G0/G1 synchronization via a 24 h DMSO 1.5 % treatment. Cells were released in the cycle, and the percentage of cells in the cell cycle phases was measured by flow cytometry.

(G) Relative incorporation of ^{14}C from Na+, ^{14}C-HCO_3^- into RNA. Labeling was performed for 6 h in HeLa cells transfected with siRNA targeting SLC4A7 or nontargeting controls to measure de novo purine and pyrimidine synthesis.

(H) Uptake of glutamine, glycine and aspartate measured in HeLa cells cultured in 10% serum and transfected with siRNA targeting SLC4A7 or nontargeting controls for 48 h. Cells were labeled with ^{14}C-glutamine, ^{14}C-glycine, or ^{14}C-aspartate over 5 min. The CPM values were normalized to the protein concentration and uptake duration. Relative levels are presented. The data are presented as the means ± SDs of two independent experiments.

(I) Schematic illustrating the fate of hypoxanthine and uridine into the nucleotide salvage pathways.

(J) Relative incorporation of ^{3}H from hypoxanthine or uridine into RNA. Labeling was performed for the last 6 h in HeLa cells transfected with siRNA targeting SLC4A7 or nontargeting controls for 48h.

$p < 0.05$, by two-tailed Student's t-test for pairwise comparisons (D, G).

Fig. S3

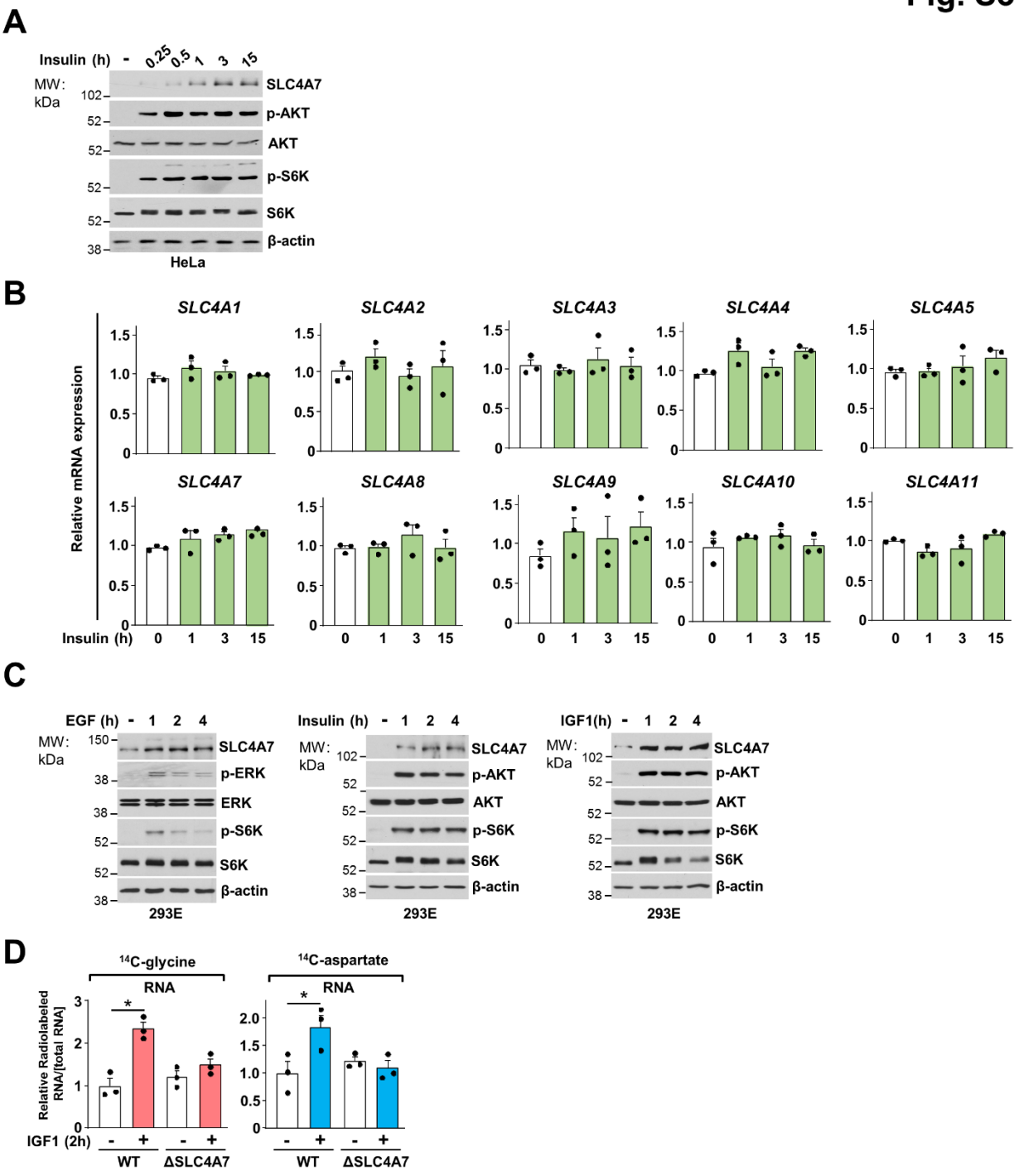

Figure S3. SLC4A7 protein abundance is stimulated by growth factors to promote nucleotide synthesis. Related to Figure 3.

(A) Acute Insulin stimulation increases SLC4A7 protein abundance. HeLa cells were stimulated with insulin over time and immunoblots were performed to assess SLC4A7 protein levels, AKT and mTORC1 signaling.

(B) Bicarbonate transporters mRNA levels, as measured by qRT-PCR, in serum-starved HeLa cells (15 h) and stimulated or not with insulin (100 nM) for the indicated times.

(C) Immunoblots from HeLa or HEK293E cells serum starved for 15 h and stimulated or not with EGF (50 ng/mL), insulin (Ins, 100 nM), or IGF1 (50 ng/mL).

(D) Relative incorporation of ^{14}C from glycine or aspartate into RNA. Wild-type or *ΔSLC4A7* HeLa cells were serum starved for 15 h and stimulated or not with IGF1 (50 ng/mL) for 3 h in the presence of the radiotracers.

*$p < 0.05$ by one-way ANOVA with Tukey's post hoc test for multiple pairwise comparisons (D).

Fig. S4

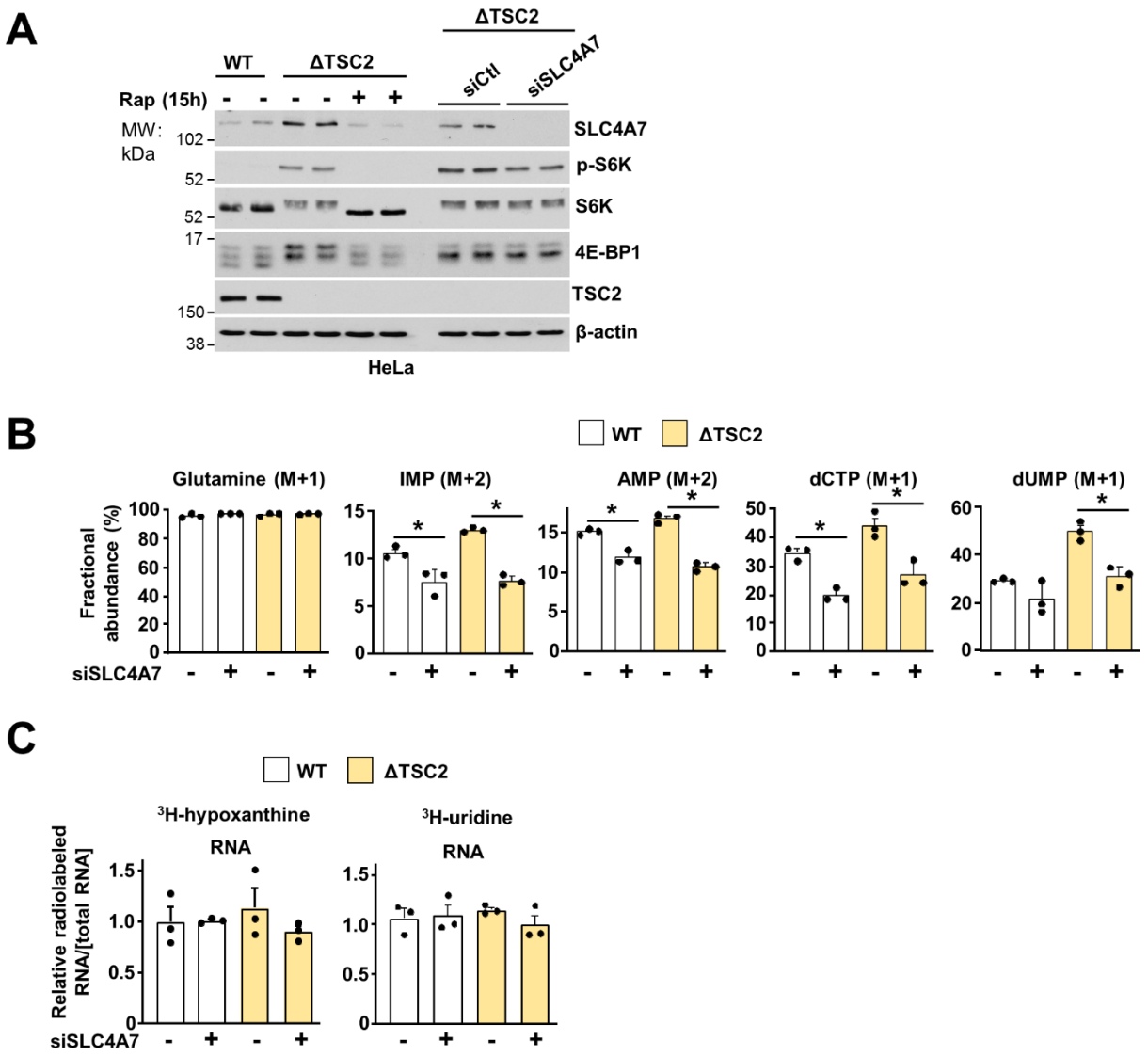

Figure S4. SLC4A7 is a downstream target of mTORC1 and is required to support de novo nucleotide synthesis but not the salvage pathway. Related to Figure 4.

(A) Immunoblots of wild-type and *ΔTSC2* HeLa cells transfected with siRNA targeting SLC4A7 or nontargeting controls for 48 h and serum starved for 15 h prior to protein extraction and SDS PAGE.

(B) Fractional abundance of ^{15}N-labeled metabolite intermediates, as measured as by LC-MS/MS, in wild-type and *ΔTSC2* HeLa cells transfected with siRNA targeting SLC4A7 or nontargeting controls for 48 h and serum starved for 15 h and labeled with ^{15}N-(amide)-glutamine for 1 h. These data support the stable-isotope tracing experiments presented in Figures 4G-I.

(C) Relative incorporation of ^{3}H from hypoxanthine or uridine into RNA. Labeling was performed for the last 6 h in wild-type and *ΔTSC2* HeLa cells transfected with siRNA targeting SLC4A7 or nontargeting controls for 48 h.

*$p < 0.05$ by a one-way ANOVA with Tukey's post hoc test for multiple pairwise comparisons (B).

Fig. S5

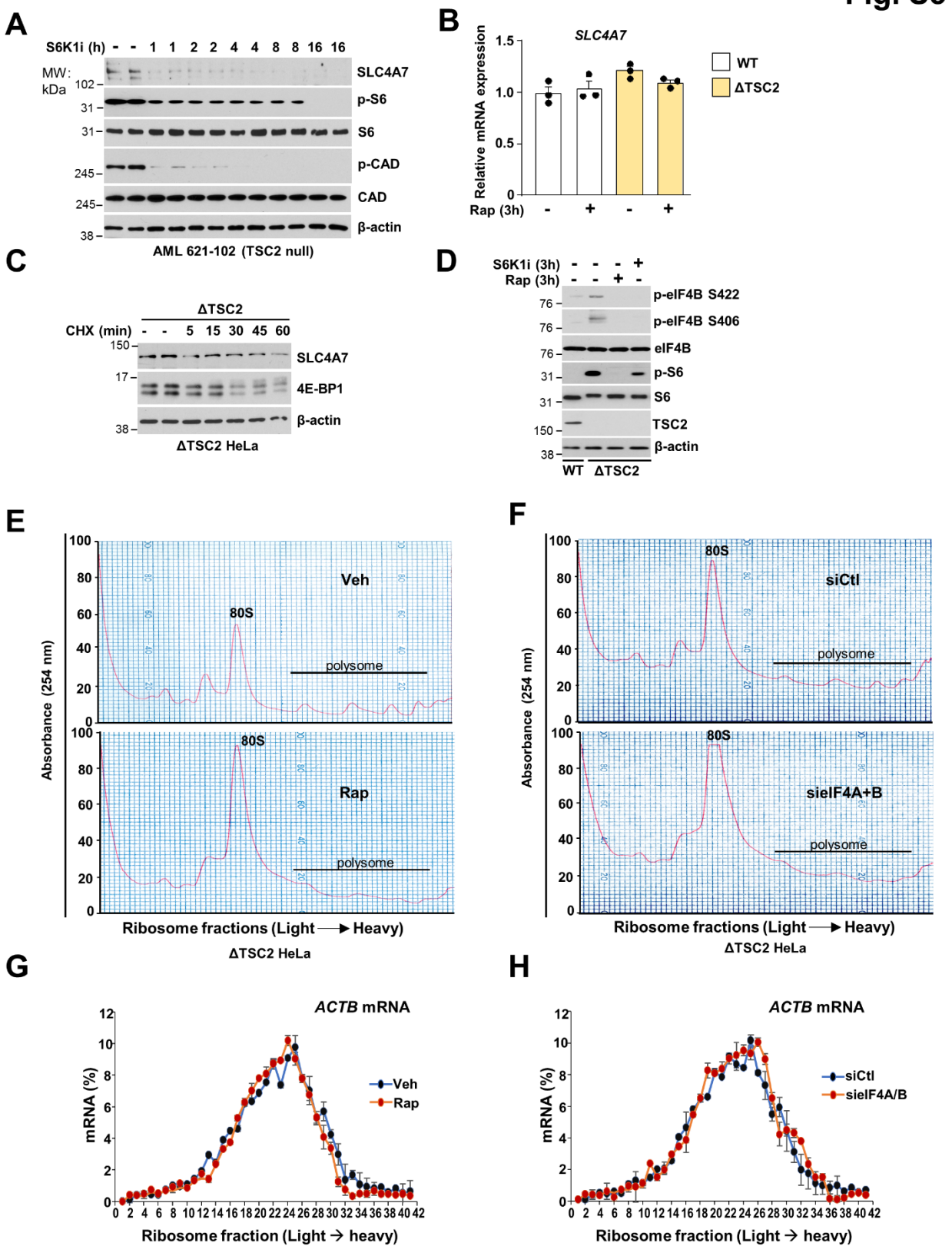
A
S6K1i (h) - - 1 1 2 2 4 4 8 8 16 16
MW: kDa
102
31
31
245
245
38
SLC4A7
p-S6
S6
p-CAD
CAD
β-actin
AML 621-102 (TSC2 null)
B
SLC4A7
Relative mRNA expression
1.5
1.0
0.5
0
WT
ΔTSC2
Rap (3h) - + - +
C
ΔTSC2
CHX (min) - - 5 15 30 45 60
150
17
38
SLC4A7
4E-BP1
β-actin
ΔTSC2 HeLa
D
S6K1i (3h) - - - +
Rap (3h) - - + -
76
76
76
31
31
150
38
p-eIF4B S422
p-eIF4B S406
eIF4B
p-S6
S6
TSC2
β-actin
WT
ΔTSC2
E
Absorbance (254 nm)
Veh
80S
polysome
Rap
80S
polysome
Ribosome fractions (Light ⟶ Heavy)
ΔTSC2 HeLa
F
Absorbance (254 nm)
siCtl
80S
polysome
sieIF4A+B
80S
polysome
Ribosome fractions (Light ⟶ Heavy)
ΔTSC2 HeLa
G
ACTB mRNA
mRNA (%)
Veh
Rap
Ribosome fraction (Light → heavy)
H
ACTB mRNA
mRNA (%)
siCtl
sieIF4A/B
Ribosome fraction (Light → heavy)

Figure S5. SLC4A7 is regulated by mTORC1 through mRNA translation-dependent mechanisms. Related to Figure 5.

(A) Immunoblot analysis of human angiomyolipoma (AML) 621-101 (*TSC2*$^{-/-}$) cells treated with vehicle (DMSO) or S6K1 inhibitor (PF-470871, 10 μM) at the indicated times.

(B) qPCR analysis of SLC4A7 expression in wild-type and *ΔTSC2* HeLa cells treated or not with vehicle (DMSO) or rapamycin (20 nM) for 3 h.

(C) Immunoblots of *ΔTSC2* HeLa cells serum starved for 15 h and treated with cycloheximide (CHX, 10 μM) at the indicated times.

(D) Immunoblots of wild-type and *ΔTSC2* HeLa cells serum starved for 15 h and treated with either vehicle (DMSO), S6K1 inhibitor (PF-470871, 10 μM), or rapamycin (20 nM) for 3 h.

(E) Sucrose-gradient analysis of polysomes from *ΔTSC2* HeLa cells treated with either vehicle or rapamycin (20 nM).

(F) Sucrose-gradient analysis of polysomes from *ΔTSC2* HeLa cells transfected with siRNAs targeting eIF4A/B or nontargeting controls.

(G) qPCR analysis of sucrose-gradient polysome fractions of *ΔTSC2* HeLa cells treated as in E.

(H) qPCR analysis of sucrose-gradient polysome fractions of *ΔTSC2* HeLa cells treated as in F.

(B, G, H) The data are graphed as the means ± SDs of biological triplicates and are representative of at least two independent experiments (B, E, F, G, H).

Fig. S6

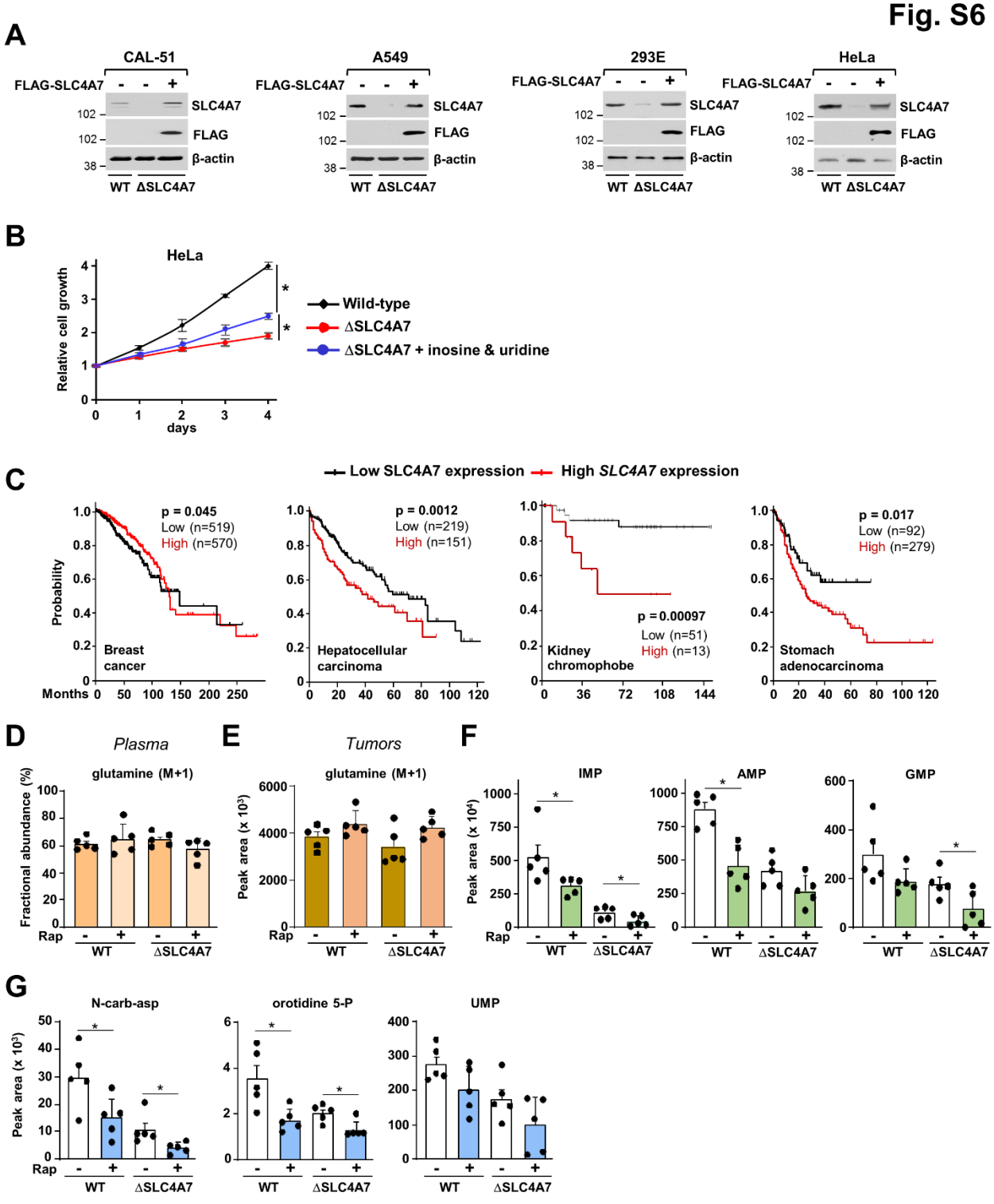

Figure S6. High expression of SLC4A7 is associated with poor survival rate in cancer patients. Related to Figure 6.

(A) Immunoblots of the indicated wild-type or ΔSLC4A7 cell lines transfected with an empty vector construct or a cDNA expressing FLAG-SLC4A7.

(B) Wild-type or ΔSLC4A7 HeLa cells were grown with 10% dialyzed serum for 96 h, in the presence of absence of inosine (200 μM) and uridine (200 μM) and cell number was measured via crystal violet staining every 24 h.

(C) Overall survival curves were generated using the database from the Human Protein Atlas based on data stratified on the best performing threshold for *SLC4A7* mRNA expression. Survival curves are plotted for all breast cancer patients (n = 1149), hepatocellular carcinoma (n = 370), kidney chromophobe (n = 64), and stomach adenocarcinoma (n = 371).

(D) Fractional enrichment of ^{15}N-glutamine in the plasma from mice bearing CAL-51-derived tumors injected intraperitoneally with ^{15}N-amide-glutamine.

(E) Normalized peak areas of ^{15}N-glutamine, measured via LC-MS/MS, from the CAL-51-derived tumors. These data support the in vivo stable-isotope tracing experiments presented in Figures 6H, I.

(F, G) Normalized peak areas of the steady-state levels of purine (F) and pyrimidine intermediates (G) from the CAL-51-derived tumors presented in Figures 6H, I.

*$p < 0.05$ by a one-way ANOVA with Tukey's post hoc test for multiple pairwise comparisons (B, F, G) or by a two-tailed Student's t-test for pairwise comparisons (C).